JUSTC

Article

http://justc.ustc.edu.cn

Received: January 22, 2025; Accepted: March 04, 2025

Sr^{2+} and choline chloride cointercalation in V_2O_5 for aqueous zinc-ion batteries

Shiyuan Chen[1], and Yongchun Zhu[1,2] ✉

[1]*School of Chemistry and Materials Science, University of Science and Technology of China, Hefei 230026, China;*
[2]*Hefei National Research Center for Physical Sciences at the Microscale, University of Science and Technology of China, Hefei 230026, China*

✉Correspondence: Yongchun Zhu, E-mail: ychzhu@ustc.edu.cn

Graphical abstract

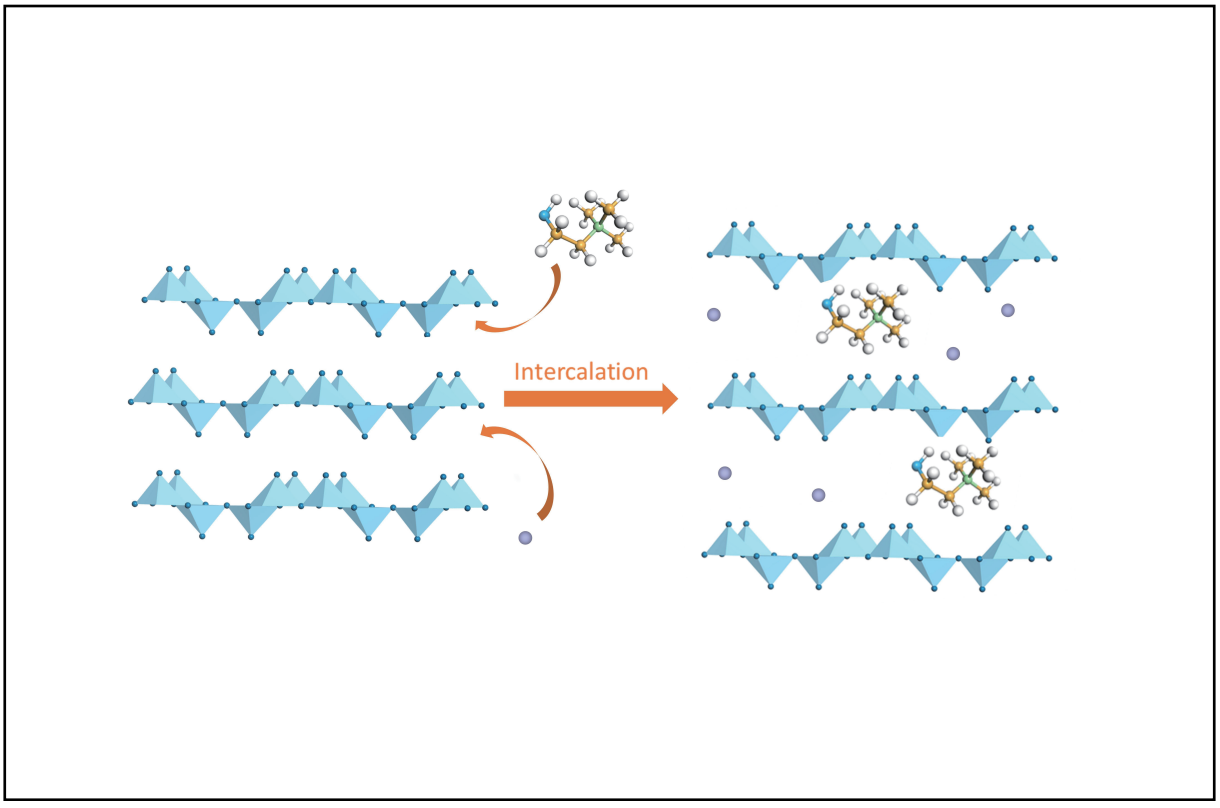

A cointercalation strategy with organic choline chloride and inorganic strontium ions is proposed to improve the performance of vanadium pentoxide as a cathode material for aqueous zinc-ion batteries, and its electrochemical performance as a cathode for aqueous zinc-ion batteries is investigated.

Public summary

- We synthesized vanadium pentoxide co-intercalated with Sr^{2+} and choline ions by a simple hydrothermal method.
- It provides new ideas for the design of cathode material structure and the application of organic-inorganic hybrid materials.
- The energy storage performance is attributed to the ability of choline ions as a wide pillar to expand the layer spacing, stabilize the layered structure of vanadium pentoxide, and strontium ions as a narrow pillar to improve ion transport kinetics, increasing capacitance contribution.

Citation: Chen S Y, Zhu Y C. Sr^{2+} and choline chloride cointercalation in V_2O_5 for aqueous zinc-ion batteries. *JUSTC*, **2025**, 55(3): 0303. CSTR: 32290.14.JUSTC-2025-0007. DOI: 10.52396/JUSTC-2025-0007

JUSTC

Article

http://justc.ustc.edu.cn

Received: January 22, 2025; Accepted: March 04, 2025

Sr^{2+} and choline chloride cointercalation in V_2O_5 for aqueous zinc-ion batteries

Shiyuan Chen[1], and Yongchun Zhu[1,2] ✉

[1]*School of Chemistry and Materials Science, University of Science and Technology of China, Hefei 230026, China;*
[2]*Hefei National Research Center for Physical Sciences at the Microscale, University of Science and Technology of China, Hefei 230026, China*

✉Correspondence: Yongchun Zhu, E-mail: ychzhu@ustc.edu.cn

Cite This: *JUSTC*, **2025**, 55(3): 0303 (7pp) Read Online SI Supporting Information

Abstract: $V_2O_5 \cdot nH_2O$ has been widely studied for aqueous zinc-ion batteries. The intercalation of inorganic ions has been used as a feasible method to improve the capacity of vanadium pentoxide. To further improve the stability, organic small molecule choline chloride intercalation is used to expand the spacing of the vanadium pentoxide layers and increase the cycling stability. Therefore, we consider the introduction of Sr^{2+} to cointercalate with choline chloride. Here, we synthesized vanadium pentoxide cointercalated with Sr^{2+} and choline ions (Ch^+) via a simple hydrothermal method. The electrochemical performance shows an enhanced cathode capacitance contribution of Sr&Ch-V_2O_5, with a discharge capacity of 526 mAh·g^{-1} at 0.1 A·g^{-1} and a retention rate of 78.9% after 2000 cycles at 5 A·g^{-1}. This work offers a novel strategy for the design of organic–inorganic hybrid materials for use as cathodes in aqueous zinc-ion batteries.

Keywords: aqueous Zn-ion batteries; vanadium oxides; ion intercalation

CLC number: TM912; TB33 **Document code:** A

1 Introduction

Aqueous rechargeable Zn-ion batteries (AZIBs) have been regarded as promising secondary chemical battery systems because of the excellent safety, low cost, and environmental friendliness[1]; these batteries have a low redox potential (−0.76 V compared with that of standard hydrogen electrodes (SHEs)) and high theoretical mass (820 mAh·g^{-1})[2]. Nonetheless, scientists still committed to develop suitable cathodes for ion insertion[1].

Layered vanadium-based materials, with an open crystal framework and large interlayer spacing[3], are available cathodes for AZIBs. However, the structural stability and ion diffusion kinetics of layered vanadium oxides need to be further improved[4].

At present, researchers have attempted to preinsert metal ions, such as K[5], Na[6], and Ca[7], to obtain vanadium pentoxide cathode materials with increased capacity. However, its cyclic stability still needs to be further improved. Moreover, researchers have successfully inserted organic ions such as polyaniline between the layers of vanadium pentoxide to alter the cyclic stability of the battery. Zhang et al.[8] modified V_2O_5 by in-situ polyaniline (PANI) intercalation to expand the layer spacing in order to gain better-performing cathodes. Inspired by the above research status, we report hydrated vanadium pentoxide with Sr^{2+} and choline ions (Ch^+) intercalation via a simple hydrothermal method. Inorganic and organic ion cointercalation improves both the capacity and cycling stability. On the one hand, the divalent earth metal ion Sr^{2+} is used between the layers to increase the capacitance contribution by increasing the number of oxygen vacancies; on the other hand, the organic choline ion is used to stabilize the layered structure of vanadium pentoxide, and improve the stability of the cycle. The vanadium pentoxide cathode of Sr^{2+} intercalation can obtain a discharge specific capacity of 338 mAh·g^{-1} at 0.2 A·g^{-1} (which of the original hydrated vanadium pentoxide is only 77 mAh·g^{-1}). The vanadium pentoxide cathode of choline chloride intercalation can still maintain a 95% capacity retention rate after 2000 cycles at a current density of 5 A·g^{-1}. Dual-intercalated hydrated vanadium pentoxide can provide a high operating voltage of 1.4 V, a capacity of 526 mA·g^{-1}, and a cycling performance of 78.9% retention after 2000 cycles at 5 A·g^{-1}. This work offers a novel strategy for the design of cathode material structures and the application of organic–inorganic hybrid materials for AZIBs.

2 Materials and methods

The synthesis method of V_2O_5 with Sr^{2+} and Ch^+ intercalation is as follows (Fig. 1a): 2 mmol of commercial V_2O_5 was dispersed in 80 mL of deionized water, and 2 mL of 30% H_2O_2 was added. After stirring for 30 min at room temperature, 0.5 mmol of $SrCl_2 \cdot 6H_2O$ and 0.5 mmol of choline chloride were added, and after continuous stirring for 30 min, the concoction was subsequently transferred to a 50 mL Teflon-lined stainless-steel autoclave, where it was maintained at a temperature of 120 °C for a duration of 6 h. Upon reaching ambient temperature following the cooling process, the precipitate was subjected to centrifugal separation followed by successive washes utilizing deionized water and anhydrous ethanol. The end product was dried in a vacuum oven at 60 °C for 12 h. For comparison, pristine V_2O_5 was prepared through the same

CSTR: 32290.14.JUSTC-2025-0007
DOI: 10.52396/JUSTC-2025-0007
JUSTC, **2025**, 55(3): 0303

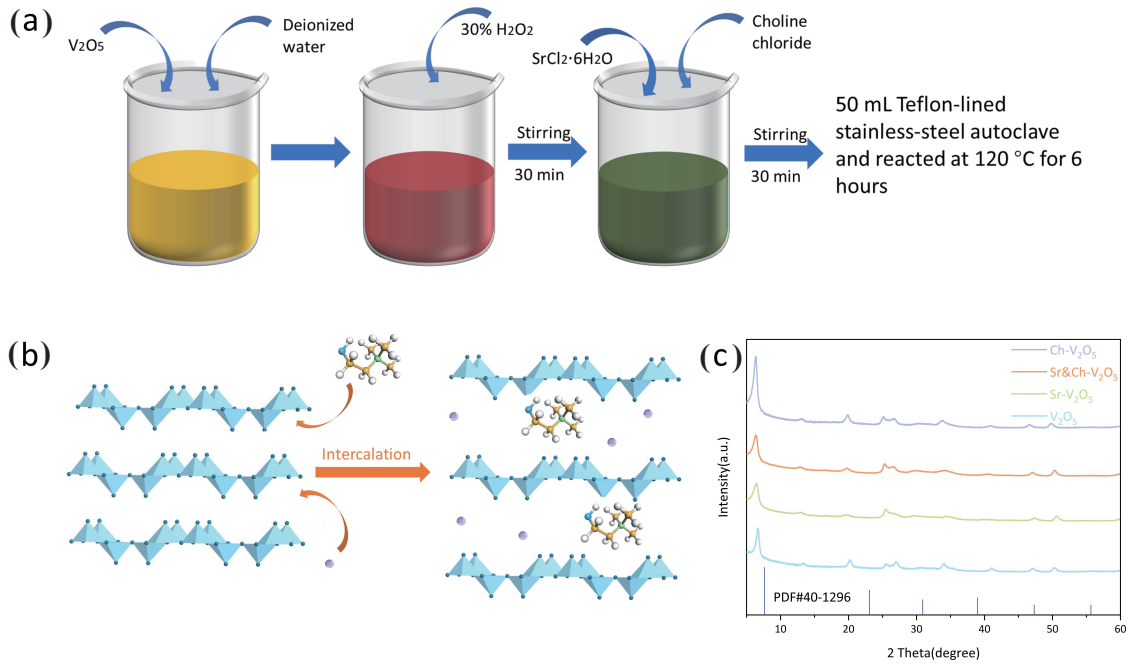

Fig. 1. Synthesis of the Sr&Ch-V_2O_5 cathode materials. (a) Schematic diagram of the synthetic route; (b) schematic diagram of the intercalation structure; (c) XRD patterns of V_2O_5, Sr&Ch-V_2O_5, Sr-V_2O_5, and Ch-V_2O_5.

process without the addition of 0.5 mmol of $SrCl_2·6H_2O$ and 0.5 mmol of choline chloride, and the same process for Sr-intercalated and Ch-intercalated V_2O_5 was used without choline chloride and $SrCl_2·6H_2O$, respectively[9].

3 Results and discussion

3.1 Structural characterization

In Fig. 1c, the XRD patterns of vanadium pentoxide in the pristine hydrate (V_2O_5), vanadium pentoxide in the Sr^{2+} intercalation (Sr-V_2O_5), vanadium pentoxide in the Ch^+ intercalation (Ch-V_2O_5), and vanadium pentoxide in the cointercalation (Sr&Ch-V_2O_5) are shown. The majority of the diffraction peaks can be attributed to the layered $V_2O_5·1.6H_2O$ structure (JCPDS No: 40-1296). After intercalation, the peak for the (001) plane of V_2O_5 shifted from 6.54° to 6.38°, implying that the lattice spacing between adjacent V–O layers expanded and that Sr^{2+} and Ch^+ successfully inserted into the V_2O_5 layer. The shift of the peak for the (001) plane of the samples with Sr^{2+} intercalation was small, whereas the shift of organic ion intercalation was large, indicating that the expansion of the layer spacing mainly depends on organic ion intercalation. The spacing of the layers of vanadium pentoxide in cointercalation is between that of Sr^{2+} intercalation and the spacing of the vanadium pentoxide layer of Ch^+ intercalation.

Fig. 2a displays the Raman spectra of individual samples, which present the characteristic peaks of $V_2O_5·1.6H_2O$. The bending vibration peak at 159 cm^{-1} is attributed to the –O–V–O–V– chains demonstrating a laminar structure, and the peak at 266 cm^{-1} is attributed to the V–O bending vibration. The peaks at 516 and 698 cm^{-1} can be related to the stretching vibrations of V_3–O and V_2–O, respectively[10]. Compared with that of pristine V_2O_5, the vibrational peak of water in the intercalated sample is significantly weakened, suggesting that the interlayer ions may replace the interlayer water molecules.

As shown in the Fourier transform infrared spectroscopy (FT-IR) spectra (Fig. 2b), the peaks located near 3420 and 1420 cm^{-1} correspond to H–O bonds, whereas the peaks at 1010, 762, and 523 cm^{-1} correspond to V–O and V=O bonds, respectively. In particular, in the spectra of the Sr&Ch-V_2O_5 and Ch-V_2O_5 samples, the peaks at 1480, 1210, and 1120 cm^{-1} represent the stretching vibration of the C–H bond and bending vibrations of the C–N and C–O bonds in Ch^+, demonstrating the insertion of ions.

The morphology of the prepared samples was characterized by scanning electron microscopy (SEM) and transmission electron microscopy (TEM). As shown in Fig. 2e, Sr&Ch-V_2O_5 displays a flower-like structure with a size of microns. In addition, scanning electron microscopy-energy dispersive spectroscopy (SEM–EDS) (Fig. 2c, d) revealed that V, O, C, N, and Sr are homogeneously distributed in the floral structure, demonstrating the uniform distribution of intercalation ions.

High-resolution TEM (HR-TEM) images (Fig. 3a) show that pristine V_2O_5 and Sr&Ch-V_2O_5 are composed of nanoribbons, and the interlayer spacing of pristine V_2O_5 is 1.304 nm. After intercalation, the lattice spacing increased to 1.332 nm in Sr-V_2O_5, 1.362 nm in Ch-V_2O_5, and 1.358 nm in Sr&Ch-V_2O_5 (Fig. 3b and Figs. S1, S2 in Supporting information). The layer spacing of Sr&Ch-V_2O_5 is expanded between those of the other two samples. This illustrates that the expansion of the interlayer spacing is due mainly to the contribution of organic ion–choline chloride intercalation.

In addition, thermogravimetric analysis was performed (Fig. S3), and the mass decay of Ch-V_2O_5 was relatively fast after heating, which was speculated to indicate that the organic intercalation of choline chloride was thermodynamically unstable and that it easily escaped from the interlayer at high temperatures.

The valence state of the element was analyzed by X-ray

CSTR: 32290.14.JUSTC-2025-0007
DOI: 10.52396/JUSTC-2025-0007
JUSTC, **2025**, 55(3): 0303

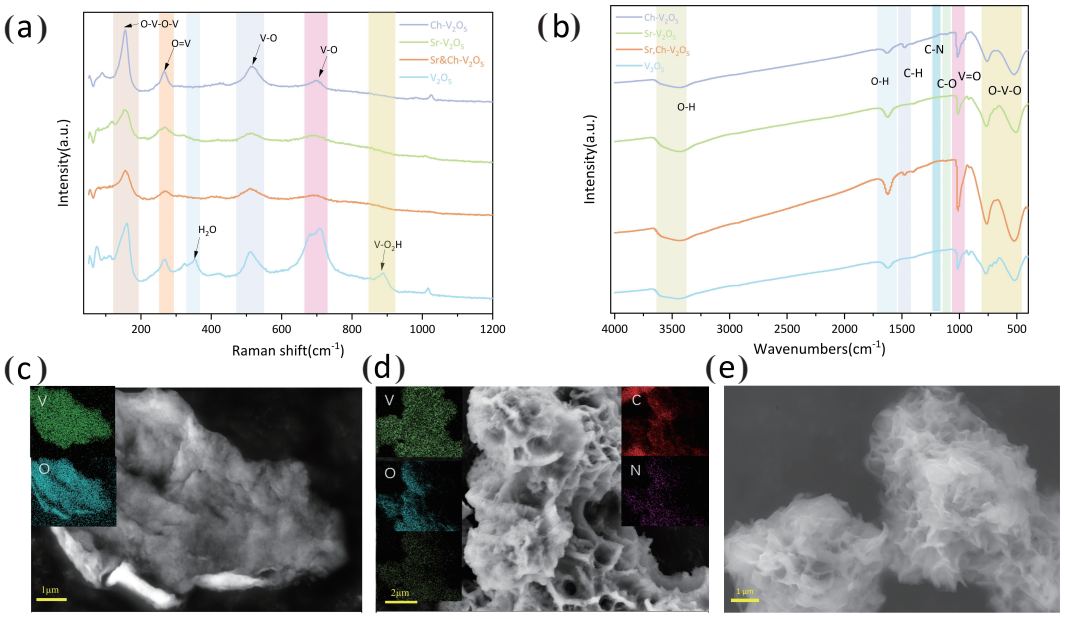

Fig. 2. Characterization of the samples. (a) Raman spectra; (b) FTIR spectra; (c, d) SEM–EDS mapping results; (e) SEM image.

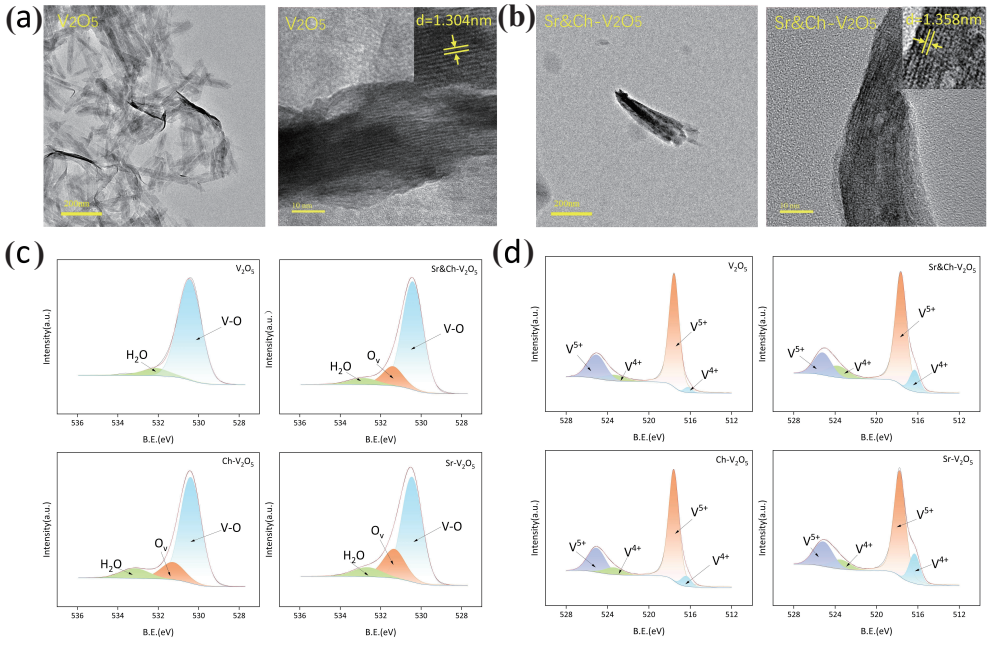

Fig. 3. Morphology and structural characterization. (a) TEM and (b) HRTEM images of V_2O_5 and Sr&Ch-V_2O_5; XPS spectra of (c) O 1 s and (d) V 2p.

photoelectron spectroscopy (XPS). The peaks of the O 1s spectrum (Fig. 3c) at 533.0 eV, 531.3 eV, and 530.4 eV correspond to structural water molecules (H_2O), oxygen vacancies (O_v) and lattice oxygen (V–O) bonds, respectively. Before discharge, compared with pristine V_2O_5, the other samples presented a higher oxygen vacancy content. Additionally, as shown in Fig. 3d, the peak of V $2p_{3/2}$ can be attributed to the amalgamation of two distinct peaks, 517.6 eV (V^{5+}) and 516.3 eV (V^{4+}). The V^{4+} content was clearly positively correlated with the number of oxygen vacancies. The increased content is caused mainly by the insertion of Sr^{2+} and Ch^{+}. The O_v content was Sr-V_2O_5>Sr&Ch-V_2O_5>Ch-V_2O_5>V_2O_5, and the relative V^{4+} content was Sr-V_2O_5>Sr&Ch-V_2O_5>Ch-V_2O_5>V_2O_5. The introduction of Sr^{2+} can cause more oxygen vacancies to appear, which can be attributed to its higher ionic valence state, resulting in a stronger interaction between Sr^{2+} and the vanadium oxygen layer.

3.2 Electrochemical properties

To delve into the electrochemical characteristics of flower-shaped Sr&Ch-V_2O_5 cathodes, it is imperative to conduct a thorough investigation. The CR2016 coin cells were assembled with zinc metal as the anode and 2 M Zn $(OTF)_2$ solution as the electrolyte. Moreover, pristine V_2O_5, Sr-V_2O_5 and Ch-V_2O_5 were used as the cathodes of the cells for comparison. Fig. 4a shows the cyclic voltammetry (CV) curve with a scan rate of 0.1 mV·s^{-1} in the range of 0.4–1.4 V potential, and it is observed that the curvilinear representation

CSTR: 32290.14.JUSTC-2025-0007
DOI: 10.52396/JUSTC-2025-0007
JUSTC, **2025**, 55(3): 0303

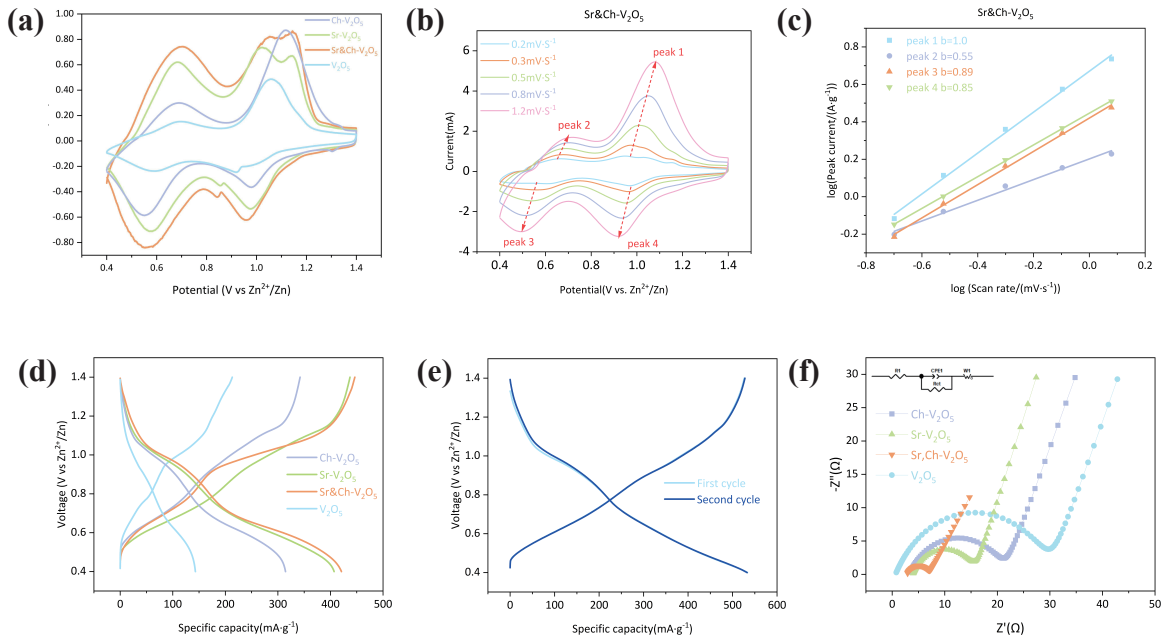

Fig. 4. Electrochemical properties. (a) CV curves; (b) CV curves at multiple scan rates of the Sr&Ch-V_2O_5 electrode; (c) log i versus log V plots of four redox peaks in the CV curves; (d) galvanostatic charge/discharge profiles at 0.1 A·g^{-1}; (e) galvanostatic charge/discharge profiles of the initial three cycles at 0.1 A g^{-1}; (f) impedance diagrams.

delineates two distinct pairs of redox peaks located at 0.62/0.52 V and 1.05/0.99 V, which correspond to the redox pair of V^{5+}/V^{4+} and V^{4+}/V^{3+}. This illustrates the existence of a multistep Zn^{2+} de/intercalation mechanism. Compared with the intercalation samples, the pristine V_2O_5 electrode has the lowest current density, the lowest capacity and the worst cycling stability. The CV curve of Sr&Ch-V_2O_5 has the highest symmetry between the oxidation and reduction curves, and its cycle reversibility is the best. The voltage gap between the V^{5+}/V^{4+} and V^{4+}/V^{3+} redox pairs of Sr&Ch-V_2O_5 indicates rapid ion diffusion and quick redox reaction kinetics. Fig. 4b shows the CV curves of the Sr&Ch-V_2O_5 electrodes at different sweep speeds. With increasing scanning rate, the configurations of diverse CV curves demonstrate a considerable degree of conformity, indicating low polarization. After the peak currents are fitted, the b values for peaks 1–4 are determined to be 1.0, 0.55, 0.89, and 0.85, respectively, according to the formula $I = av^b$. v represents the scan rate (mV·s^{-1}), a and b are alterable parameters, and the value of b ranges from 0.5 to 1.0. When b changes from 0.5 to 1, the proportion of the surface capacitance process increases, and the proportion of the diffusion-controlled process decreases[9]. On this basis, it can be concluded that there are both diffusion and capacitance behaviors in the storage of Zn^{2+}. The b value of peak 1 is 1.0, reflecting a mainly capacitive process, and the b value of peak 2 is close to 0.5, which suggests that the reaction is mostly diffusion controlled. Under the same conditions, the magnitude of the b parameter of Sr&Ch-V_2O_5 exceeded that observed in the other comparator samples, and the capacitance contribution of the Sr&Ch-V_2O_5 samples reached 66.55% at 0.6 mV·s^{-1} (Fig. S4), indicating that it had a high surface capacitance charge storage capacity and accelerated reaction kinetics. The introduction of Sr^{2+} ions increased the proportion of capacitive behavior of the vanadium pentoxide electrodes. This facilitates quick kinetic behavior and appropriate pseudocapacitance behavior, which results in superior rate performance of the cell.

The galvanostatic charge/discharge (GCD) profiles for each sample electrode during initial cycling are shown in Fig. 4d. The capacity of the samples after intercalation increased to varying degrees. The typical charge/discharge curves for the first two cycles of the Sr&Ch-V_2O_5 electrodes almost coincide with each other (Fig. 4e), which illustrates the reversibility of Zn^{2+} insertion/extraction behavior, as well as the specific capacity of 526 mAh·g^{-1} obtained at 0.1 A·g^{-1}.

After the initial activation of three cycles at a current density of 0.1 A·g^{-1}, electrochemical impedance spectroscopy (EIS) was performed on the electrodes prepared from each sample (Fig. 4f). After that, the electrochemical kinetics of the electrodes were further revealed via the galvanostatic intermittent titration technique (GITT). The apparent zinc ion diffusion coefficient $D_{Zn^{2+}}$ of the Sr&Ch-V_2O_5 electrode, calculated from the GITT curve, is approximately 10^{-9} cm^2·s^{-1} (Fig. 5d), which is much greater than that of the V_2O_5 electrode piece (10^{-10} cm^2·s^{-1}), indicating that proper layer spacing and a suitable wide and narrow column distribution between layers can lead to higher ion diffusion kinetics. The $D_{Zn^{2+}}$ of the pole piece of the single-intercalated sample also showed varying degrees of improvement.

The long-term cycling performance of the electrode prepared for each sample was tested at current densities of 0.2 and 5 A·g^{-1} (Fig. 5a, c). The electrode with a single insertion of organic ions Sr^{2+} has a good initial specific capacity of 338 mAh·g^{-1}, but the capacity retention rate is less than 70% after 45 cycles. The positive electrode of Ch-V_2O_5 can obtain a capacity retention rate of 95% after 2000 cycles at a current density of 5 A·g^{-1} but only at a lower specific capacity. Electrodes with a single insertion of the inorganic ions Sr^{2+} and the

CSTR: 32290.14.JUSTC-2025-0007
DOI: 10.52396/JUSTC-2025-0007
JUSTC, **2025**, 55(3): 0303

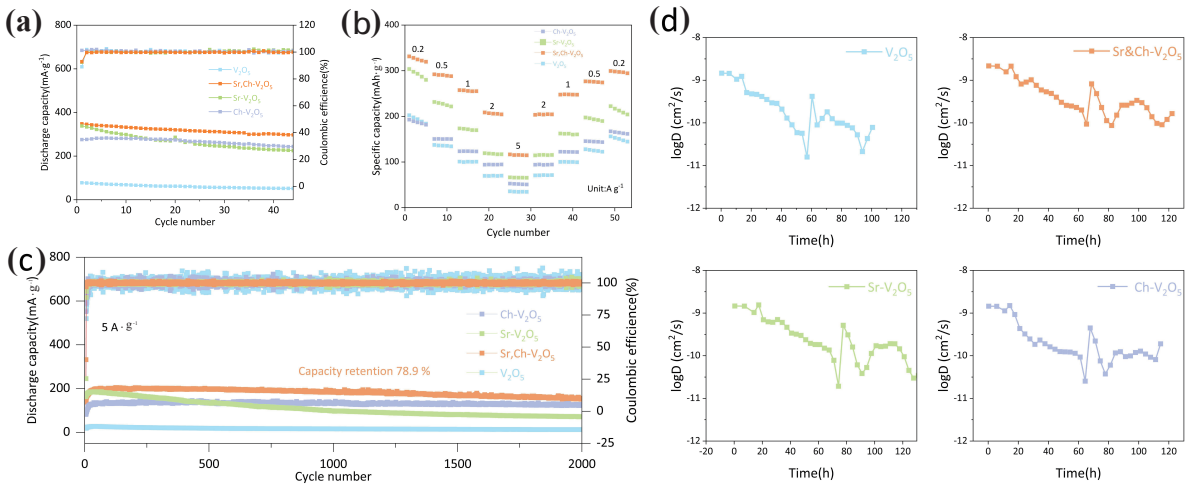

Fig. 5. Electrochemical performance. (a) Cycling performance at 0.2 A·g^{-1} for 45 cycles; (b) rate capability at various current densities (from 0.2 to 5 A·g^{-1}); (c) cycling performance at 5 A·g^{-1} for 2000 cycles; (d) Zn^{2+} diffusion coefficients.

organic ions Ch^+ have the problems of rapid specific capacity decay and low specific capacity, respectively. After the initial three activated cycles at a current density of 0.1 A·g^{-1}, the Sr&Ch-V_2O_5 maintained a good capacity retention rate of 78.9% after 2000 cycles at a current density of 5 A·g^{-1}. At a current density of 0.2 A·g^{-1}, it can maintain a specific capacity of 297.6 mAh·g^{-1} after 45 cycles. The introduction of Sr^{2+} increases the oxygen vacancy content of vanadium pentoxide, which increases the proportion of pseudocapacitance and increases the specific cycle capacity[11], and the introduction of Ch^+ stabilizes the layered structure and improves the cycling stability[8].

To verify the effect of the electrolyte on the battery cycle performance, we also used 2 M $ZnSO_4$ as the electrolyte and found that the capacity decayed rapidly, probably due to the dissolution of vanadium oxides in the 2 M $ZnSO_4$ solution (Fig. S5).

3.3 Structural stability before and after cycling

Ex situ XRD characterization was performed to study the structural stability before and after cycling. Fig. 6a and Figs. S6, S7, and S8 show the ex situ XRD diffraction patterns of the positive electrode piece before cycling, at 10 revolutions to 0.4 V, and at 10 cycles to 1.4 V. The additional diffraction peaks come from the stainless steel mesh. Fig. 6 shows the XRD diffraction patterns of the cointercalation material before and after charging and discharging. The (001) peak shifts slightly from 6.90° to 7.14° during discharging, indicating the contraction of the interlayer spacing caused by the electrostatic interaction between Zn^{2+} and O^{2-}. The (001) peak gradually

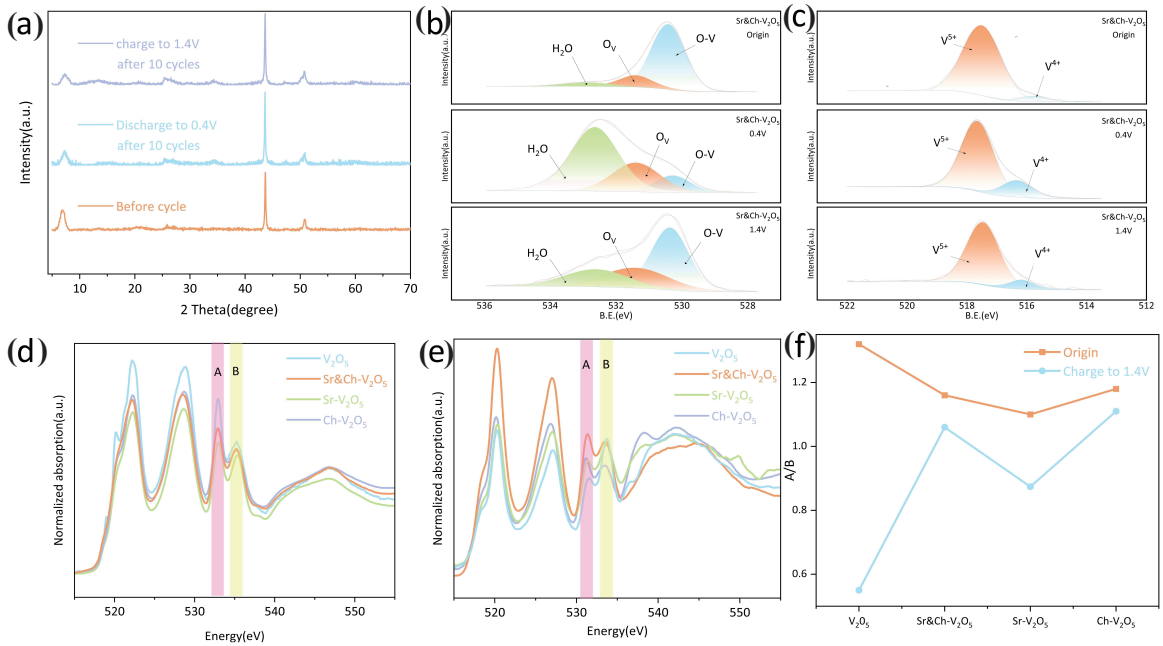

Fig. 6. (a) Ex situ XRD patterns of the Sr&Ch-V_2O_5 electrode at 1A·g^{-1} after 10 cycles; XPS of (b) O 1s and (c) V 2p spectra of the Sr&Ch-V_2O_5 cathode in the original, fully discharged and charged states, respectively; (d, e) O K-edge X-ray absorption spectra of different samples in the original and charged states; (f) ratio of peak intensities of A and B in (d) and (e).

CSTR: 32290.14.JUSTC-2025-0007
DOI: 10.52396/JUSTC-2025-0007
JUSTC, **2025**, 55(3): 0303

weakened during the discharge process, indicating that the electrostatic interaction between Zn^{2+} ions led to shrinkage of the layer spacing and weakening of the layered structure, resulting in a change in the crystal volume and an increase in lattice chaos. When recharging to 1.4 V, the intensity and position of the peaks returned to near the initial state, indicating good reversibility. Compared with that of the original vanadium pentoxide, the structural stability of the intercalated vanadium pentoxide as a cathode before and after cycling was improved. The sample with Ch^+ intercalation provides the best stability.

The valence state of the element and its change during charging/discharging were investigated via ex situ XPS (Fig. 6b, c). When discharged to 0.4 V, the intensity of the V^{5+} peak decreases, and the intensity of the V^{4+} peak increases. After being fully charged again, V^{5+} returns to a near-initial state, indicating its high reversibility.

Furthermore, we analyzed the changes in the number of oxygen vacancies before and after cycling via X-ray absorption spectroscopy (XAS). O K-edge XANES measurements were conducted to probe the electronic structure of oxygen in a charge state of 1.4 V and a discharge state of 0.4 V. In the O K-edge XAS spectra, the two peaks at ~530 and 532 eV, labeled A and B, correspond to the t_{2g} and e_g orbitals[12,13], respectively (Fig. 6d, e). Specifically, the t_{2g} peak originates from the electronic transition from O 1s to V 3d hybridized with O 2p π orbitals, whereas the e_g peak is associated with the electronic transition from O 1s to V 3d–O 2p σ orbital overlap[14,15]. The orbital splitting of oxygen is due mainly to electrostatic interactions with transition metal ions, and the relative intensities of peaks A and B in Fig. 6d and Fig. 6e reflect the relative amount of V^{4+} in the sample. The ratios of the intensities of peaks A and B in the XAS spectra of different sample preparations for different states are presented in Fig. 6f. A lower value of A/B represents a higher V^{4+} content, which also means a higher oxygen vacancy content. It can be inferred that the introduction of Sr^{2+} can increase the number of oxygen vacancies in vanadium pentoxide, which leads to an increase in the electrochemical activity, ion transport, and capacity of the electrode[16,17]. After charging to 1.4 V again, the contents of V^{4+} in V_2O_5 and Sr-V_2O_5 cannot return to the initial state level, suggesting that their cycling stability is weak. This may be due to the easy detachment of Sr^{2+} between the layers, which leads to dissolution of the vanadium pentoxide skeleton, and the introduction of Ch^+ increases the stability of the interlayer structure of vanadium pentoxide.

4 Conclusions

In summary, we proposed a cointercalation strategy to improve the performance of vanadium pentoxide as a cathode material for aqueous zinc-ion batteries, prepared Sr&Ch-V_2O_5 with choline chloride and strontium chloride as intercalation raw materials via a simple hydrothermal method, and investigated its role as a cathode for aqueous zinc-ion batteries. The excellent energy storage performance is attributed to the ability of choline ions to expand the layer spacing and stabilize the layered structure of vanadium pentoxide and strontium ions to increase the amount of oxygen vacancies to improve the capacitance contribution and ion transport kinetics.

Supporting information

The supporting information for this article can be found online at https://doi.org/10.52396/JUSTC-2025-0007. The supporting information includes an experimental section, XPS spectra, SEM images, TEM images, TG curves, and electrochemical performances.

Acknowledgements

We acknowledge the support from the beam-lines BL11U, BL10B, and BL12B-a of National Synchrotron Radiation Laboratory (NSRL, Hefei, China).

Conflict of interest

The authors declare that they have no conflict of interest.

Biographies

Shiyuan Chen is currently a graduate student in the School of Chemistry and Materials Science, University of Science and Technology of China, under the suppervision of Prof. Yongchun Zhu. Her research mainly focuses on the modification strategies of vanadium pentoxide cathodes of aqueous zinc-ion batteries.

Yongchun Zhu is currently an Associate Professor of Chemistry and Materials Science at the University of Science and Technology of China (USTC). She received her Ph.D. degree from USTC in 2006. Her research interests include aqueous ion batteries and metal ion batteries.

References

[1] Yi T F, Qiu L Y, Qu J P, et al. Towards high-performance cathodes: Design and energy storage mechanism of vanadium oxides-based materials for aqueous Zn-ion batteries. *Coordination Chemistry Reviews*, **2021**, *446*: 214124.

[2] Gong Y X, Wang B, Ren H Z, et al. Recent advances in structural optimization and surface modification on current collectors for high-performance zinc anode: principles, strategies, and challenges. *Nano-Micro Letters*, **2023**, *15*: 208.

[3] Wang L, Zheng J. Recent advances in cathode materials of rechargeable aqueous zinc-ion batteries. *Materials Today Advances*, **2020**, *7*: 100078.

[4] Zhou T, Zhu L M, Xie L L, et al. Cathode materials for aqueous zinc-ion batteries: A mini review. *Journal of Colloid and Interface Science*, **2022**, *605*: 828–850.

[5] Li H P, Zhao R Z, Zhou W H, et al. Trade-off between zincophilicity and zincophobicity: toward stable Zn-Based aqueous batteries. *JACS Au*, **2023**, *3* (8): 2107–2116.

[6] Liu H, Jiang L, Cao B, et al. Van der Waals interaction-driven self-assembly of V_2O_5 nanoplates and MXene for high-performing zinc-ion batteries by suppressing vanadium dissolution. *ACS Nano*, **2022**, *16* (9): 14539–14548.

[7] Liu N, Li B, He Z X, et al. Recent advances and perspectives on vanadium- and manganese-based cathode materials for aqueous zinc ion batteries. *Journal of Energy Chemistry*, **2021**, *59*: 134–159.

[8] Zhang Y F, Xu L, Jiang H M, et al. Polyaniline-expanded the interlayer spacing of hydrated vanadium pentoxide by the interface-intercalation for aqueous rechargeable Zn-ion batteries. *Journal of*

CSTR: 32290.14.JUSTC-2025-0007
DOI: 10.52396/JUSTC-2025-0007
JUSTC, **2025**, 55(3): 0303

Colloid and Interface Science, **2021**, *603*: 641–650.

[9] Zong Q, Zhuang Y L, Liu C F, et al. Dual effects of metal and organic ions co-intercalation boosting the kinetics and stability of hydrated vanadate cathodes for aqueous zinc-ion batteries. *Advanced Energy Materials*, **2023**, *13* (31): 2301480.

[10] Zhang M Y, Zhang X Q, Dong Q, et al. Organic molecularintercalated $V_3O_7{\cdot}H_2O$ with high operating voltage for long cycle life aqueous Zn-ion batteries. *Advanced Functional Materials*, **2023**, *33* (31): 2213187.

[11] Qi Y, Huang J H, Yan L, et al. Towards high-performance aqueous zinc-ion battery via cesium ion intercalated vanadium oxide nanorods. *Chemical Engineering Journal*, **2022**, *442*: 136349.

[12] Shi Y C, Chen Y, Shi L, et al. An overview and future perspectives of rechargeable zinc batteries. *Small*, **2020**, *16* (23): 2000730.

[13] Niu H H, Liu H, Yang L, et al. Impacts of distorted local chemical coordination on electrochemical performance in hydrated vanadium pentoxide. *Nature Communications*, **2024**, *15*: 9421.

[14] Chen J A, Hou X J, Wang X L, et al. Bi-intercalated vanadium pentoxide synthesized via hydrogen peroxide-induced phase transition for highly stable cathode in aqueous zinc ion batteries. *Journal of Materials Chemistry A*, **2024**, *12*: 11322–11331.

[15] Wang W F, Zhang L, Duan Z A, et al. Joint cationic and anionic redox chemistry in a vanadium oxide cathode for zinc batteries achieving high energy density. *Carbon Energy*, **2024**, *6* (11): e577.

[16] Jia X, Tian R, Liu C, et al. Stability and kinetics enhancement of hydrated vanadium oxide via sodium-ion pre-intercalation. *Materials Today Energy*, **2022**, *28*: 101063.

[17] Liu F, Chen Z X, Fang G Z, et al. V_2O_5 nanospheres with mixed vanadium valences as high electrochemically active aqueous zinc-ion battery cathode. *Nano-Micro Letters*, **2019**, *11*: 25.

CSTR: 32290.14.JUSTC-2025-0007
DOI: 10.52396/JUSTC-2025-0007
JUSTC, **2025**, 55(3): 0303